current issues in molecular biology

MDPI

Article

Oral and Intranasal Administration of Polydeoxyribonucleotide Isolated from *Porphyra* sp. Ameliorates Acute Lung Injury via Suppressing Proinflammatory Cytokine Production in Mice

Ga-Young Lee [1], Won Se Lee [2,3], Jisung Han [2,3] and Yung-Choon Yoo [1,*]

[1] Department of Microbiology, College of Medicine, Konyang University, Daejeon 32992, Republic of Korea; jc0012003@naver.com
[2] All In One GENETECH Ltd., Busan 46508, Republic of Korea; wslee8607@aiogenetech.com (W.S.L.); aio@aiogenetech.com (J.H.)
[3] DERMARE Co., Ltd., Busan 48480, Republic of Korea
* Correspondence: yc_yoo@konyang.ac.kr; Tel.: +82-42-600-8694

Abstract

Acute lung injury (ALI) is a severe inflammatory condition with high mortality rates, necessitating the development of effective therapeutic agents. Polydeoxyribonucleotide (PDRN), a DNA-derived compound known for its tissue repair and anti-inflammatory properties, has gained attention as a potential therapeutic agent. However, the efficacy of PDRN derived from marine sources, particularly *Porphyra* sp. (laver), remains unexplored in respiratory inflammation. In this study, we investigated the protective effects of *Porphyra* sp.-derived PDRN (Ps-PDRN) against LPS-induced ALI in mice through two administration routes: intranasal (IN) and oral (PO). Ps-PDRN treatment significantly attenuated fever, pulmonary edema, and histopathological changes in LPS-challenged mice. Both IN and PO administration of Ps-PDRN markedly reduced proinflammatory cytokines (TNF-α, IL-1β, and IL-6) and chemokines (MCP-1, RANTES, CXCL1, and MIP-2) in bronchoalveolar lavage fluid (BALF) and serum. Comparative analysis of the two administration routes revealed distinct efficacy profiles, with oral administration demonstrating superior chemokine inhibition, while intranasal delivery showed advantages in certain cytokine suppression. Histological examination revealed that Ps-PDRN preserved alveolar architecture and reduced inflammatory cell infiltration. Furthermore, in vitro studies using RAW 264.7 macrophages demonstrated that Ps-PDRN inhibited LPS-induced production of proinflammatory cytokines, such as TNF-α and IL-6, in a dose-dependent manner. These findings suggest that Ps-PDRN exerts potent anti-inflammatory effects against ALI through both local and systemic administration routes, highlighting its potential as a novel therapeutic agent for inflammatory lung diseases.

Keywords: *Porphyra* sp.; polydeoxyribonucleotide; PDRN; acute lung injury; inflammation; cytokines; chemokines; administration route

Academic Editor: Chan-Yen Kuo

Received: 31 December 2025
Revised: 28 January 2026
Accepted: 29 January 2026
Published: 6 February 2026

1. Introduction

Acute lung injury (ALI) and its more severe manifestation, acute respiratory distress syndrome (ARDS), are fatal inflammatory syndromes marked by widespread alveolar damage, pulmonary edema, and progressive respiratory failure [1]. Despite advances in critical care medicine, ALI remains associated with significant morbidity and mortality, with limited therapeutic options available [2]. The pathogenesis of ALI involves complex

inflammatory cascades triggered by various insults, including bacterial infections, where lipopolysaccharide (LPS) from Gram-negative bacteria plays a pivotal role in initiating and amplifying the inflammatory response [3,4].

LPS activates alveolar macrophages and epithelial cells by binding to its receptor toll-like receptor 4 (TLR4) on the cells, and triggers the release of a panel of proinflammatory cytokines—tumor necrosis factor-α (TNF-α), interleukin-1β (IL-1β), and interleukin-6 (IL-6)—alongside chemokines, including monocyte chemoattractant protein-1 (MCP-1) and macrophage inflammatory protein-2 (MIP-2) [5,6]. These inflammatory mediators promote neutrophil recruitment, increase vascular permeability, and cause tissue damage, ultimately leading to impaired gas exchange and respiratory failure [5]. Therefore, therapeutic strategies targeting excessive inflammatory responses represent a promising approach for ALI management. Polydeoxyribonucleotide (PDRN) is a mixture of deoxyribonucleotide polymers included in various biological sources, typically salmon sperm [7]. Clinical applications of PDRN include treatment of chronic wounds, osteoarthritis, and various inflammatory conditions [8,9]. However, most studies have focused on PDRN derived from salmon (*Oncorhynchus* spp.), and the therapeutic potential of PDRN from alternative marine sources remains largely unexplored.

Porphyra sp., commonly known as laver or nori, is a marine red algae widely consumed as a traditional food in East Asian countries [10]. This edible seaweed is rich in bioactive compounds, including polysaccharides, proteins, and nucleic acids [11]. Recent advances in extraction technology have enabled the isolation of PDRN from *Porphyra* sp., yielding a mixture of polydeoxyribonucleotide and polynucleotide with a molecular weight range of 5–1000 kDa [12]. Prior PDRN evidence is largely based on salmon-derived preparations and injection-based administration, highlighting the need for studies assessing alternative marine sources and non-invasive delivery routes (Supplementary Table S1). Given the abundant availability and sustainable cultivation of *Porphyra* sp., this marine-derived PDRN represents a promising alternative source for therapeutic applications [13]. In our recent work, we showed that *Porphyra* sp.-derived PDRN (Ps-PDRN) exerts anti-inflammatory activity in LPS-stimulated RAW 264.7 macrophages by reducing nitric oxide (NO) production, which was accompanied by suppression of MAPK signaling, including ERK and p38 activation [14].

In this study, we investigated the inhibitory effects of Ps-PDRN on ALI in an in vivo mouse model and analyzed the related immunological mechanisms in lung tissue. Notably, we compared two administration routes—intranasal (IN) and oral (PO)—to evaluate both local and systemic therapeutic approaches. Additionally, we examined the in vitro anti-inflammatory activity of Ps-PDRN using LPS-stimulated RAW 264.7 macrophages. Our findings provide the first evidence for the protective effects of *Porphyra* sp.-derived PDRN against ALI, suggesting its potential as a novel therapeutic agent for inflammatory lung diseases.

2. Materials and Methods

2.1. Ps-PDRN Manufacturing Process

Ps-PDRN was prepared following previously reported procedures with minor wording revision [12,14]. In brief, *Porphyra* sp. was washed three times under running tap water to remove attached epiphytes, residual salts, and sand, and was then thoroughly rinsed with fresh water. The cleaned material was stored at −20 °C until further processing. After freeze-drying, the samples were finely homogenized to obtain a dry powder.

The powdered *Porphyra* sp. was lysed using a protein lysis buffer consisting of 10 wt% soybean, 10 wt% adlay, 20 wt% green tea extract, 20 wt% soybean fatty acid, 20 wt% tocopherol, cocamidopropyl betaine, and 20 wt% olive oil carboxylate. Subse-

quently, ribonucleases were added to facilitate the separation of polynucleotides and PDRN. The lysate was cleared by centrifugation and filtration to eliminate insoluble debris and other contaminants. The resulting filtrate was dried, washed, and centrifuged to recover the low-molecular-weight Ps-PDRN fraction. The final preparation was concentrated by evaporation and lyophilized to yield Ps-PDRN powder, which was stored at −80 °C until use. Purity was evaluated by the absorbance ratio at 260/280 nm (A260/A280), and DNA concentration was calculated from A260 using a microplate reader (PowerWave XS2, BioTek Instruments, Inc., Winooski, VT, USA). The purity of the isolated Ps-PDRN was ≥99% as previously described [12]. The protein content of Ps-PDRN was not detected by the BCA assay kit (Thermo Fisher Scientific, Waltham, MA, USA), and the endotoxin content was less than 0.005 EU/mL when measured by the LAL chemical production assay kit (Lonza, Walkersville, MD, USA).

2.2. Cell Culture and Cytotoxicity Assay

RAW 264.7 murine macrophages were purchased from the Korean Cell Line Bank (Seoul, Republic of Korea). Cells were maintained in DMEM supplemented with 10% fetal bovine serum (FBS) and 1% penicillin–streptomycin at 37 °C in a humidified incubator with 5% CO. To evaluate the cytotoxicity of Ps-PDRN, an MTT assay was performed. Cells were plated in 96-well culture plates at a density of 5×10^4 cells/well and allowed to attach for 8 h. The cells were then exposed to Ps-PDRN at the indicated concentrations (0–100 μg/mL) for 12 h, followed by LPS challenge (1 μg/mL; *Escherichia coli* serotype 055:B5, Sigma-Aldrich, St. Louis, MO, USA) for an additional 24 h. Next, MTT solution (5 mg/mL) was added and incubated for 2 h. After centrifugation, the supernatant was carefully discarded, and the resulting formazan crystals were solubilized in dimethyl sulfoxide (DMSO). Absorbance was read at 540 nm using a microplate reader.

2.3. Determination of Cytokines in Cell Culture

For cytokine measurements, RAW 264.7 cells were pre-incubated with Ps-PDRN at the specified concentrations for 12 h and subsequently stimulated with LPS (100 ng/mL) for 24 h. Culture supernatants were collected, and TNF-α and IL-6 concentrations were determined using commercial ELISA kits (BD Biosciences, San Jose, CA, USA) according to the manufacturer's protocol.

2.4. Real-Time PCR Analysis

Total RNA was extracted from RAW 264.7 cells or lung tissues using TRIzol reagent (iNtRON Biotechnology, Seongnam, Republic of Korea). cDNA was synthesized using a power cDNA synthesis kit (iNtRON Biotechnology), and quantitative real-time PCR was performed using Cfx96 (Bio-Rad, Hercules, CA, USA). The expression levels of TNF-α, IL-1β, and IL-6 were normalized to GAPDH. The primer sequences are listed in Table 1.

Table 1. Primer sequences for quantitative real-time PCR analysis.

Gene	Primer Sequence (5′ → 3′)	Accession No.	Catalog No.
TNF-α	F: GGTGCCTATGTCTCAGCCTCTT R: GCCATAGAACTGATGAGAGGGAG	NM_013693	MP217748
IL-1β	F: TGGACCTTCCAGGATGAGGACA R: GTTCATCTCGGAGCCTGTAGTG	NM_008361	MP206724
IL-6	F: TACCACTTCACAAGTCGGAGGC R: CTGCAAGTGCATCATCGTTGTTC	NM_031168	MP206798
GAPDH	F: CATCACTGCCACCCAGAAGACTG R: ATGCCAGTGAGCTTCCCGTTCAG	NM_008084	MP205604

All primers were obtained from OriGene Technologies, Inc. (Rockville, MD, USA). F, forward primer; R, reverse primer.

2.5. Animal Experiments

Seven-week-old male BALB/c mice (19–22 g) were obtained from Raon Bio (Yongin, Republic of Korea). All animal procedures were performed in compliance with institutional animal care guidelines and were approved by the Animal Ethics Committee of Konyang University (Approval No. P-25-12-A-01). Mice were randomly divided into seven groups (n = 7 per group): (1) normal control; (2) LPS (vehicle); (3) LPS + dexamethasone (DEX, 5 mg/kg/mouse, positive control); (4) LPS + Ps-PDRN IN-Low (IN-L, 25 μg/mouse); (5) LPS + Ps-PDRN IN-High (IN-H, 50 μg/mouse); (6) LPS + Ps-PDRN PO-Low (PO-L, 100 μg/mouse); and (7) LPS + Ps-PDRN PO-High (PO-H, 200 μg/mouse). For intranasal administration groups, Ps-PDRN was administered intranasally once daily for three days before ALI induction. For the oral administration regimen, Ps-PDRN was delivered by gavage once daily for three consecutive days prior to ALI induction. Acute lung injury was then established by intranasal instillation of LPS (100 μg/mouse). Eighteen hours after the LPS challenge, mice were euthanized, and lung tissues, whole blood, and bronchoalveolar lavage fluid (BALF) were harvested for subsequent analyses.

2.6. Body Temperature and Lung Edema Assessment

Body temperature was measured using a rectal thermometer 24 h after LPS administration. For lung edema assessment, lungs were excised, weighed (wet weight), and dried in an oven at 60 °C for 48 h to obtain dry weight. The wet/dry (W/D) ratio was calculated as an indicator of pulmonary edema.

2.7. BALF and Serum Analysis

BALF was collected by lavaging the lungs three times with 1 mL of cold PBS. Blood was collected by cardiac puncture and centrifuged to obtain serum. The concentrations of cytokines (TNF-α, IL-1β, and IL-6) and chemokines (MCP-1, RANTES, CXCL1, and MIP-2) in BALF and serum were measured using ELISA kits (BD Biosciences) according to the manufacturer's protocols.

2.8. Histological Analysis

Lung tissues were fixed in 4% paraformaldehyde (Image-IT™ Fixative Solutions; Invitrogen, Waltham, MA, USA), cryoprotected by immersion in 30% sucrose, and embedded in Tissue-Tek OCT compound (Sakura Finetek USA Inc., Torrance, CA, USA). Cryosections were cut using a cryostat (CM1520; Leica Biosystems, Nussloch, Germany) and subsequently stained with hematoxylin and eosin (H&E) for histopathological evaluation. Additionally, BALF cells were cytospun onto glass slides and stained with Diff-Quik for morphological analysis of alveolar macrophages. Images were captured using a light microscope (BX53; Olympus, Hachioji-shi, Tokyo, Japan) at 20× (lung tissue) or 200× (macrophage) magnification.

2.9. Histopathological Quantitative Image Analysis

Morphometric analysis was performed using ImageJ software (version 1.54, National Institutes of Health, Bethesda, MD, USA) according to previously established methods [1,2]. For each animal, five non-overlapping random fields per section were analyzed by an investigator blinded to group assignment. Alveolar Air Space Ratio: Digital images were converted to 8-bit grayscale, and a threshold was applied to distinguish air-filled spaces (white) from tissue (dark).

The alveolar air space ratio was calculated as follows:

Alveolar Air Space Ratio (%) = (Air space area/Total lung area) × 100 Tissue Cellularity:

Color deconvolution was applied to separate the hematoxylin (purple/blue, nuclei) channel. After thresholding, the tissue cellularity was calculated as follows:

$$\text{Tissue Cellularity (\%)} = (\text{Purple-stained cellular area}/\text{Total lung area}) \times 100$$

2.10. BALF Alveolar Macrophage Analysis

Cytospin preparations of BALF cells were stained with Diff-Quik and analyzed for macrophage morphometry. For each animal, at least 50 macrophages from five random high-power fields (HPF, 200× magnification) were evaluated.

Mean Macrophage Size: After scale calibration, individual macrophages were outlined using the freehand selection tool, and cross-sectional areas (μm^2) were measured. Alveolar macrophages typically range between 15 and 21 μm in diameter under resting conditions, with increased size indicating cellular activation [3].

Macrophage Count: The number of macrophages per HPF was counted using the Cell Counter plugin in ImageJ. At least five non-overlapping HPFs were counted per animal [4].

2.11. Statistical Analysis

Data are presented as mean ± standard deviation (SD). Statistical analyses were conducted using SAS 9.4. For experiments involving three or more groups, differences among groups were assessed using one-way analysis of variance (ANOVA) followed by an appropriate post hoc multiple-comparison test. Specifically, when comparing each treatment group against the LPS group, Dunnett's post hoc test was used; when all pairwise comparisons were required, Tukey's HSD was applied. For comparisons that involved both administration route (oral vs. intranasal) and dose, a two-way ANOVA was performed to evaluate the main effects of route and dose as well as their interaction (route × dose), followed by post hoc multiple comparisons with multiplicity control.

Normality and homoscedasticity assumptions were evaluated where applicable; when assumptions were not met, the Mann–Whitney U test (two-group comparisons) or Kruskal–Wallis test with a suitable post hoc procedure (multiple groups) was applied. A p-value < 0.05 was considered statistically significant. Where relevant, adjusted p-values are reported for multiple comparisons.

For descriptive cross-marker comparisons of route-specific efficacy, percent inhibition rates were calculated as [(LPS − Treatment)/(LPS − Normal)] × 100. Effect sizes were estimated using Cohen's d with 95% confidence intervals to quantify the magnitude of treatment effects relative to the LPS group. These inhibition-rate and effect-size analyses were treated as supportive/illustrative and are presented in the Supplementary Materials (heatmap, radar chart, and forest plot). Supplementary analyses and visualizations were performed using SAS 9.4 and Orange 3.

3. Results

3.1. Ps-PDRN Attenuates LPS-Induced Fever and Pulmonary Edema

Intranasal administration of LPS induced significant increases in body temperature (from 35.8 °C to 38.0 °C) and lung wet/dry ratio in mice, indicating the successful establishment of the ALI model (Figure 1). Treatment with Ps-PDRN via both IN and PO routes significantly reduced the LPS-induced elevation in body temperature. The IN-L (25 μg/mouse) and IN-H (50 μg/mouse) groups showed body temperatures comparable to the dexamethasone-treated group. Interestingly, both PO-L (100 μg/mouse) and PO-H (200 μg/mouse) groups showed significant antipyretic effects. Pulmonary edema, assessed by the lung W/D ratio, was markedly increased following the LPS challenge. Both IN and PO administration of Ps-PDRN significantly reduced the W/D ratio in a dose-dependent

manner, with the PO-L group showing the most pronounced effect (Figure 1B). Comparative analysis revealed that oral administration achieved 56.3% inhibition of pulmonary edema compared to 39.8% for intranasal administration (Supplementary Figure S1). These results indicate that Ps-PDRN effectively ameliorates systemic inflammation and pulmonary edema associated with ALI.

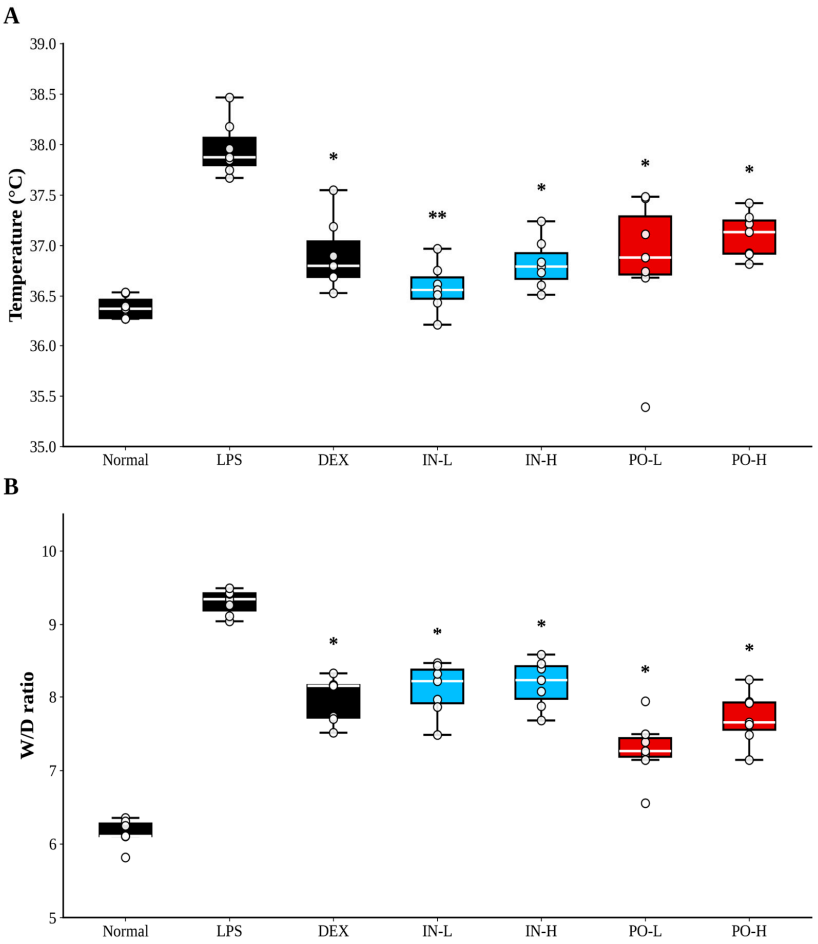

Figure 1. Ps-PDRN attenuates LPS-induced fever and pulmonary edema: (**A**) body temperature; (**B**) lung wet/dry (W/D) ratio. Data are presented as mean ± SD (n = 7). One-way ANOVA followed by Dunnett's multiple-comparison test (each treatment vs. the LPS group) was used. * $p < 0.05$, ** $p < 0.01$ vs. LPS group.

3.2. Ps-PDRN Reduces Proinflammatory Cytokines in BALF

LPS administration markedly elevated the concentrations of proinflammatory cytokines such as TNF-α, IL-1β, and IL-6 in BALF (Figure 2). Treatment with Ps-PDRN via both routes significantly suppressed these cytokine levels. For TNF-α, all treatment groups showed significant reductions compared to the LPS group, with the IN-H group demonstrating the most potent inhibition (Figure 2A). IL-1β levels were significantly reduced in all Ps-PDRN-treated groups, with PO-L showing comparable efficacy to dexamethasone (Figure 2B). IL-6 concentrations were also markedly decreased in both IN and PO groups, with intranasal administration showing superior efficacy (83.3% inhibition) compared to oral administration (59.7% inhibition) (Figure 2C; Supplementary Figure S2).

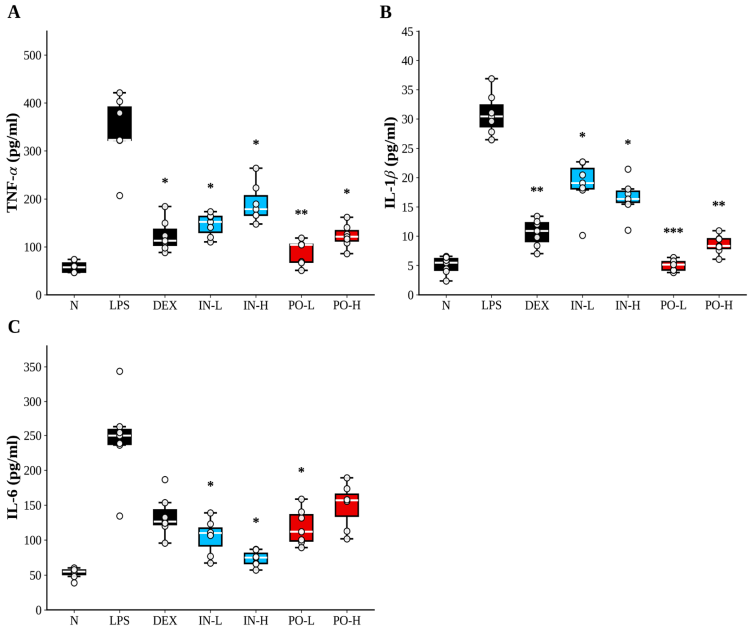

Figure 2. Effects of Ps-PDRN on proinflammatory cytokine levels in BALF: (**A**) TNF-α; (**B**) IL-1β; (**C**) IL-6. Data are presented as mean ± SD (n = 7). One-way ANOVA followed by Dunnett's multiple-comparison test (each treatment vs. the LPS group) was used. * $p < 0.05$, ** $p < 0.01$, *** $p < 0.001$ vs. LPS group.

3.3. Ps-PDRN Reduces Cytokine mRNA Expression in Lung Tissues

To examine the effects of Ps-PDRN at the transcriptional level, we analyzed the mRNA expression of proinflammatory cytokines in lung tissues by real-time PCR (Figure 3). LPS challenge significantly upregulated TNF-α, IL-1β, and IL-6 mRNA expression compared to the normal control group. Both IN and PO administration of Ps-PDRN markedly suppressed the mRNA levels of these cytokines. Notably, dexamethasone treatment almost completely abolished TNF-α and IL-6 mRNA expression, while Ps-PDRN treatment showed significant but partial inhibition. For IL-1β, all treatment groups demonstrated comparable efficacy in reducing mRNA expression.

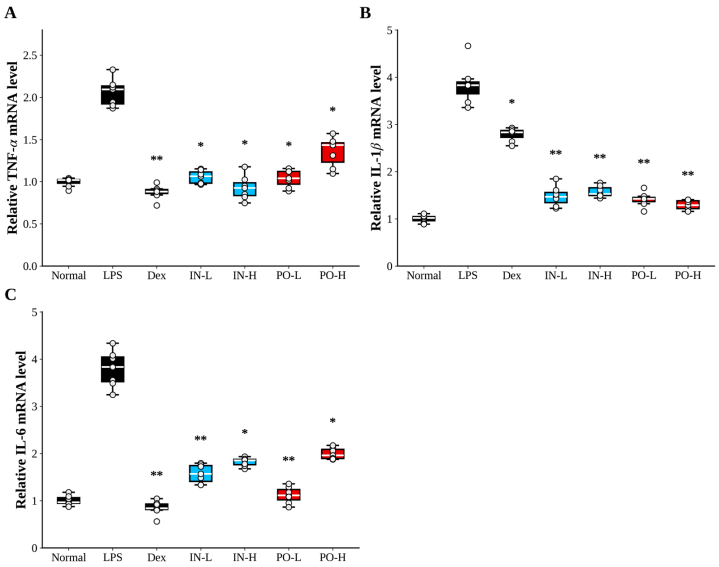

Figure 3. Effects of Ps-PDRN on cytokine mRNA expression in lung tissues: (**A**) TNF-α; (**B**) IL-1β; (**C**) IL-6. mRNA levels were measured by real-time PCR and normalized to GAPDH. Data are presented as mean ± SD (n = 7). One-way ANOVA followed by Dunnett's multiple-comparison test (each treatment vs. the LPS group) was used. * $p < 0.05$, ** $p < 0.01$ vs. LPS group.

3.4. Ps-PDRN Reduces Chemokine Levels in BALF

Chemokines play crucial roles in recruiting inflammatory cells to the lungs during ALI. We measured the levels of MCP-1, RANTES (CCL5), CXCL1, and MIP-2 in BALF (Figure 4). LPS administration dramatically increased the concentrations of all four chemokines compared to the normal group. Ps-PDRN treatment reduced MCP-1, RANTES, CXCL1, and MIP-2 levels in both intranasal (IN) and oral (PO) administration groups. Overall, the PO groups showed a stronger suppression trend across chemokines, and the PO-L condition exhibited near-complete normalization for MCP-1 and MIP-2 relative to the LPS group (Supplementary Figure S1). Notably, the dose–response pattern suggested that lower oral dosing can achieve robust chemokine suppression, highlighting a potential dose-dependent window that warrants confirmation in dedicated therapeutic (post-insult) studies. Notably, the PO-L condition (100 μg/mouse) exhibited robust suppression of MCP-1 and MIP-2 levels. However, the observed non-linear dose–response pattern for oral administration warrants cautious interpretation, as it may reflect differences in absorption/processing, biological saturation, or variability in systemic distribution rather than definitive dose superiority. Further dose-optimization and pharmacokinetic studies are required to elucidate the oral dose–response relationship.

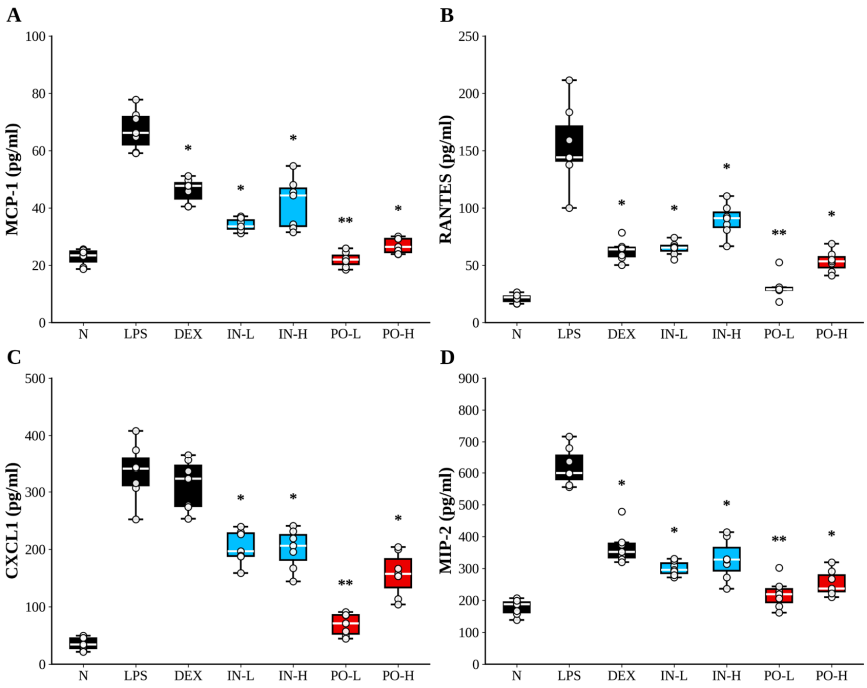

Figure 4. Effects of Ps-PDRN on chemokine levels in BALF: (**A**) MCP-1; (**B**) RANTES; (**C**) CXCL1; (**D**) MIP-2. Data are presented as mean ± SD (n = 7). One-way ANOVA followed by Dunnett's multiple-comparison test (each treatment vs. the LPS group) was used. * $p < 0.05$, ** $p < 0.01$ vs. LPS group.

3.5. Ps-PDRN Ameliorates Histopathological Changes in Lung Tissues

Histological examination of lung tissues revealed that LPS administration caused severe pathological changes, including inflammatory cell infiltration, thickening of alveolar septa, and destruction of alveolar architecture (Figure 5). In contrast, treatment with Ps-PDRN via both IN and PO routes markedly attenuated these histopathological alterations. The alveolar structure was better preserved in Ps-PDRN-treated groups, with reduced inflammatory cell infiltration comparable to the dexamethasone-treated group.

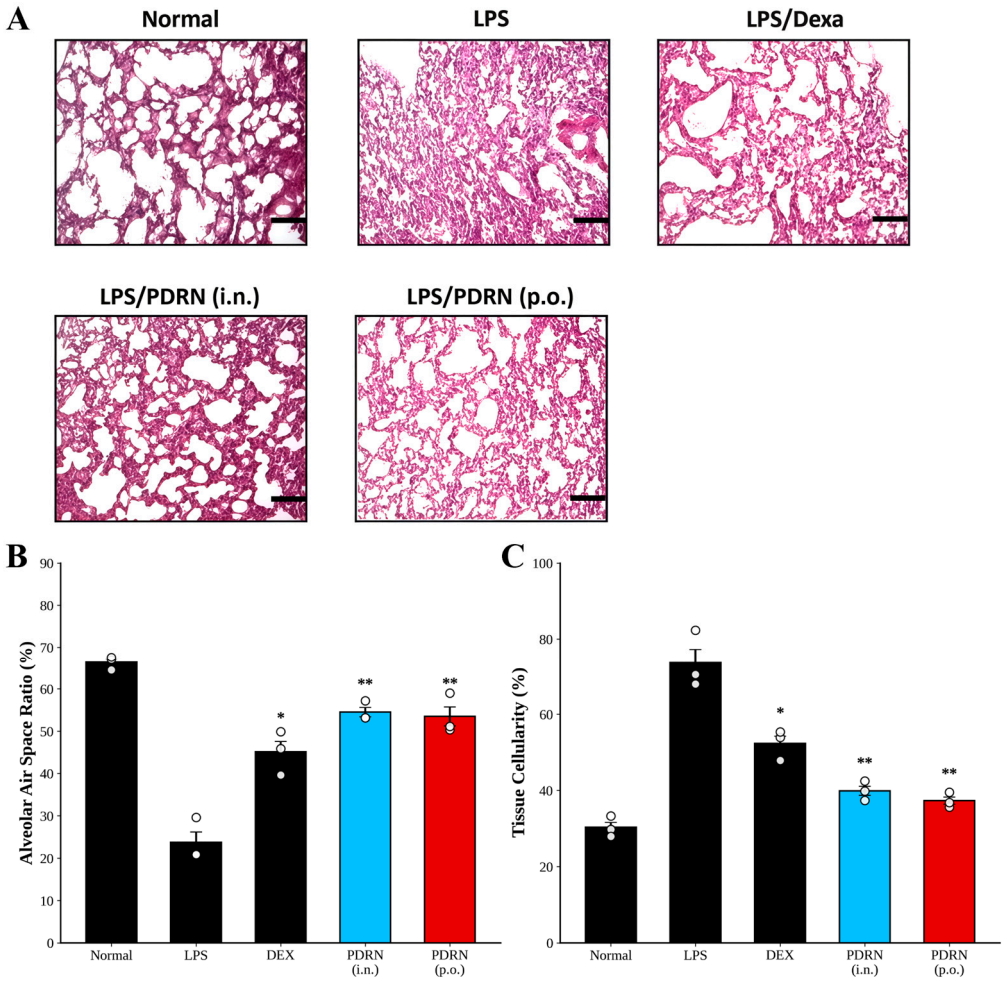

Figure 5. Histopathological analysis of lung tissues: (**A**) Representative hematoxylin-and-eosin (H&E)-stained lung sections from each experimental group. Normal control shows an intact alveolar structure with thin alveolar septa. LPS group exhibits severe inflammatory cell infiltration, alveolar wall thickening, and reduced air space. The LPS/Dexa (dexamethasone, 3 mg/kg) group shows partial attenuation of lung injury. LPS/PDRN (i.n.) (intranasal, 50 mg/mouse) and LPS/PDRN (p.o.) (oral, 200 mg/mouse) groups demonstrate preserved alveolar architecture with markedly reduced inflammatory cell infiltration. Scale bar = 100 µm. (**B**) Quantitative analysis of alveolar air space ratio. The percentage of air-filled alveolar space was measured using ImageJ software. (**C**) Quantitative analysis of tissue cellularity. The percentage of cellular (purple-stained) area was measured using ImageJ software. Data are presented as mean ± SEM (n = 3). Statistical analysis was performed using one-way ANOVA followed by Tukey's HSD post hoc test. * $p < 0.05$, ** $p < 0.01$ vs. LPS group.

3.6. Effects of Ps-PDRN on Alveolar Macrophage Activation

Cytological examination of BALF cells revealed distinct morphological changes in alveolar macrophages following LPS challenge (Figure 6). In the LPS group, alveolar macrophages exhibited activated morphology characterized by increased cell size and vacuolization. Treatment with Ps-PDRN reduced the activated morphology of alveolar macrophages, although some degree of activation remained, similar to the dexamethasone-treated group.

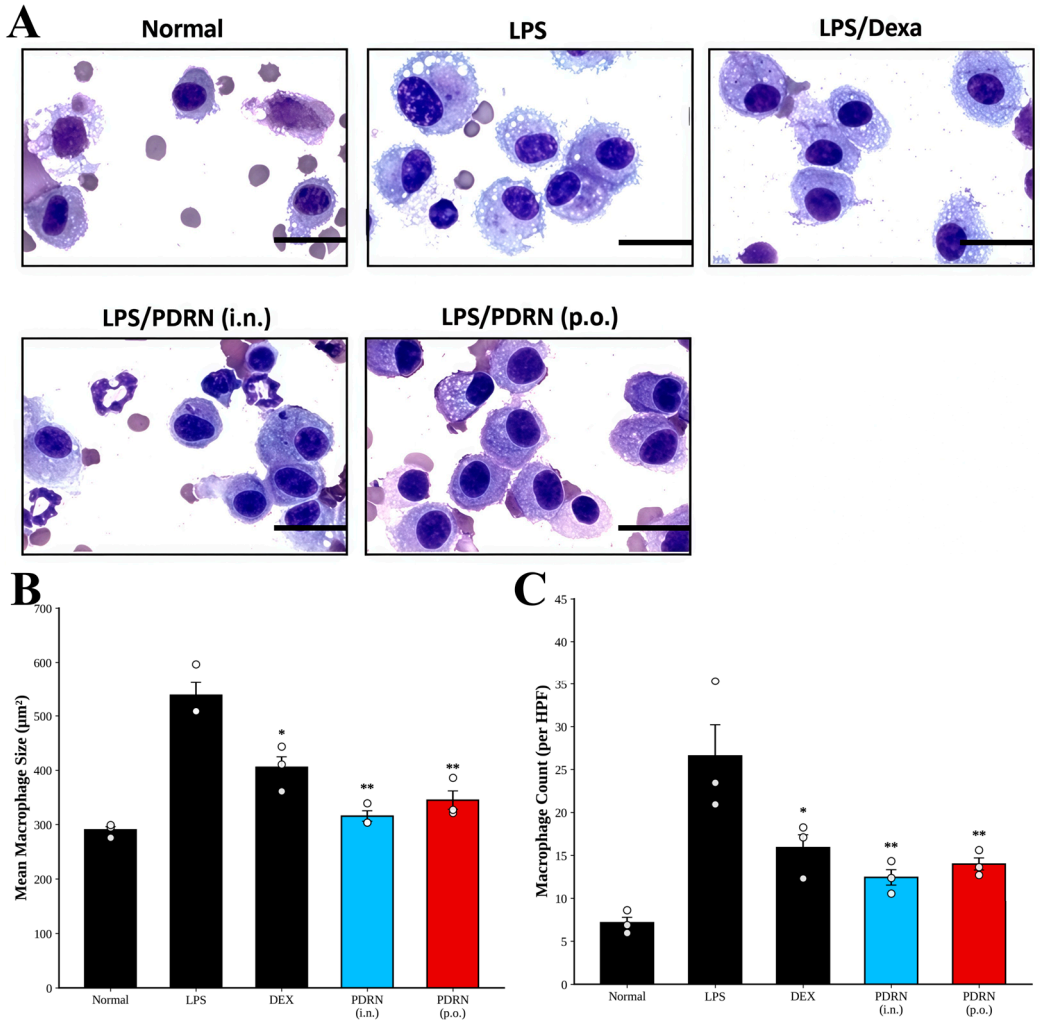

Figure 6. Morphological analysis of alveolar macrophages in bronchoalveolar lavage fluid (BALF): (**A**) Representative cytospin images of BALF cells stained with Diff-Quik. Normal control shows small, round resting macrophages. LPS group demonstrates enlarged, activated macrophages with spread morphology and vacuolated cytoplasm. LPS/Dexa group shows partial reduction in macrophage activation. LPS/PDRN (i.n., 50 mg/mouse) and LPS/PDRN (p.o., 200 mg/mouse) groups exhibit reduced macrophage size and activation comparable to the Dexa group. Scale bar = 10 μm. (**B**) Mean macrophage cross-sectional area (μm^2) measured by ImageJ analysis. (**C**) Macrophage count per high-power field (HPF, 400×). A minimum of 50 macrophages per animal from five random HPFs were analyzed by a blinded observer. Data are presented as mean ± SEM (n = 3 per group). Statistical analysis was performed using one-way ANOVA followed by Tukey's HSD post hoc test. * $p < 0.05$, ** $p < 0.01$ vs. LPS group.

3.7. Ps-PDRN Reduces Serum Inflammatory Markers

To evaluate the systemic anti-inflammatory effects of Ps-PDRN, we measured cytokine and chemokine levels in serum (Figure 7). LPS challenge significantly elevated serum levels of TNF-α, IL-6, MCP-1, and MIP-2. Both IN and PO administration of Ps-PDRN significantly reduced these inflammatory markers. Interestingly, the two administration routes showed distinct efficacy profiles for serum markers: intranasal administration demonstrated superior efficacy in reducing TNF-α (67.0% vs. 51.1% inhibition) and IL-6 (45.5% vs. 30.9% inhibition), while oral administration showed better results for MCP-1 (90.9% vs. 68.2% inhibition) and MIP-2 (86.7% vs. 68.7% inhibition) (Supplementary Figures S2 and S4). These results indicate that Ps-PDRN exerts systemic anti-inflammatory effects with route-specific advantages.

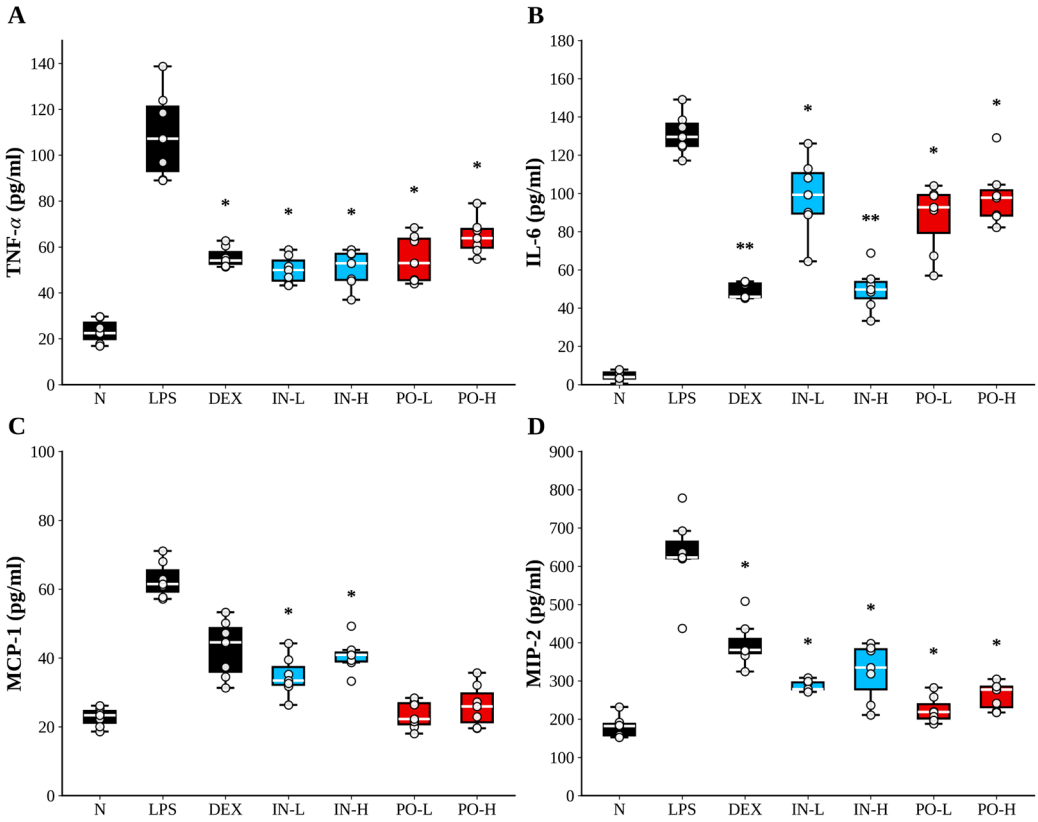

Figure 7. Effects of Ps-PDRN on serum cytokine and chemokine levels: (**A**) TNF-α; (**B**) IL-6; (**C**) MCP-1; (**D**) MIP-2. Data are presented as mean ± SD (n = 7). One-way ANOVA followed by Dunnett's multiple-comparison test (each treatment vs. the LPS group) was used. * $p < 0.05$, ** $p < 0.01$ vs. LPS group.

3.8. Ps-PDRN Inhibits Inflammatory Responses in RAW 264.7 Macrophages

To investigate the direct anti-inflammatory effects of Ps-PDRN on macrophages, we performed in vitro experiments using RAW 264.7 cells. Based on our previous findings that Ps-PDRN inhibits NO production in LPS-stimulated RAW 264.7 macrophages [14], we investigated its inhibitory effects on inflammatory cytokine (TNF-α and IL-6) production here. First, we assessed the cytotoxicity of Ps-PDRN using the MTT assay. Ps-PDRN showed no significant cytotoxicity up to 100 μg/mL in both LPS-stimulated and unstimulated conditions (Figure 8A), although a slight reduction in cell viability was observed at the highest concentration (100 μg/mL) in LPS-stimulated cells. Treatment with Ps-PDRN dose-dependently inhibited LPS-induced production of TNF-α and IL-6 in RAW 264.7 cells (Figure 8B,C). At 25 μg/mL, Ps-PDRN reduced TNF-α production by approximately 40% compared to the LPS control. At 50 μg/mL, TNF-α levels were further reduced to approximately 30% of the LPS control levels. Similarly, IL-6 production was significantly inhibited by Ps-PDRN treatment, with the most pronounced effect observed at 50 μg/mL.

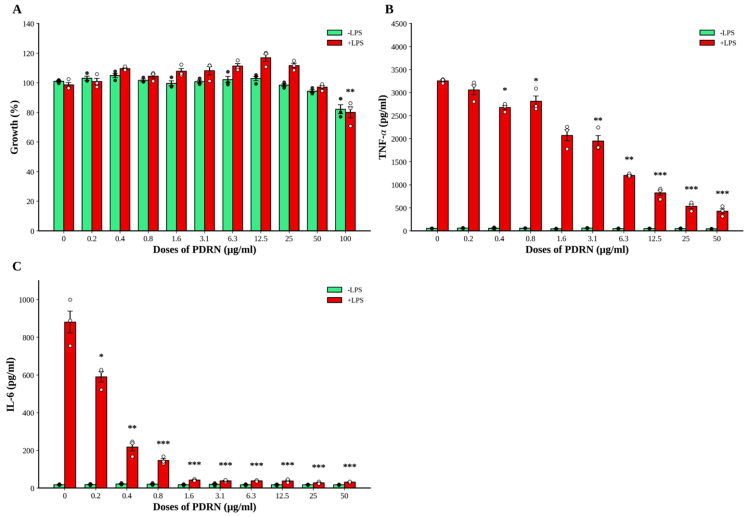

Figure 8. In vitro effects of Ps-PDRN on RAW 264.7 macrophages: (**A**) cell viability assessed by MTT assay; (**B**) TNF-α production; (**C**) IL-6 production. Cells were pretreated with Ps-PDRN for 12 h and stimulated with LPS (1 μg/mL) for 24 h. Data are presented as mean ± SD (n = 3). Two-way ANOVA (LPS × dose) was performed. Post hoc comparisons were conducted using Dunnett's test within the LPS condition only, comparing each Ps-PDRN dose to LPS + 0 μg/mL. * $p < 0.05$, ** $p < 0.01$, *** $p < 0.001$ vs. LPS group.

3.9. Ps-PDRN Suppresses Cytokine mRNA Expression in RAW 264.7 Cells

Real-time PCR analysis confirmed that Ps-PDRN suppressed the mRNA expression of proinflammatory cytokines in LPS-stimulated RAW 264.7 cells (Figure 9). LPS stimulation dramatically increased TNF-α, IL-1β, and IL-6 mRNA levels. Treatment with Ps-PDRN (10 and 20 μg/mL) significantly reduced the mRNA expression of all three cytokines in a dose-dependent manner. At 20 μg/mL, Ps-PDRN reduced TNF-α, IL-1β, and IL-6 mRNA levels by approximately 95%, 90%, and 95%, respectively, compared to the LPS control.

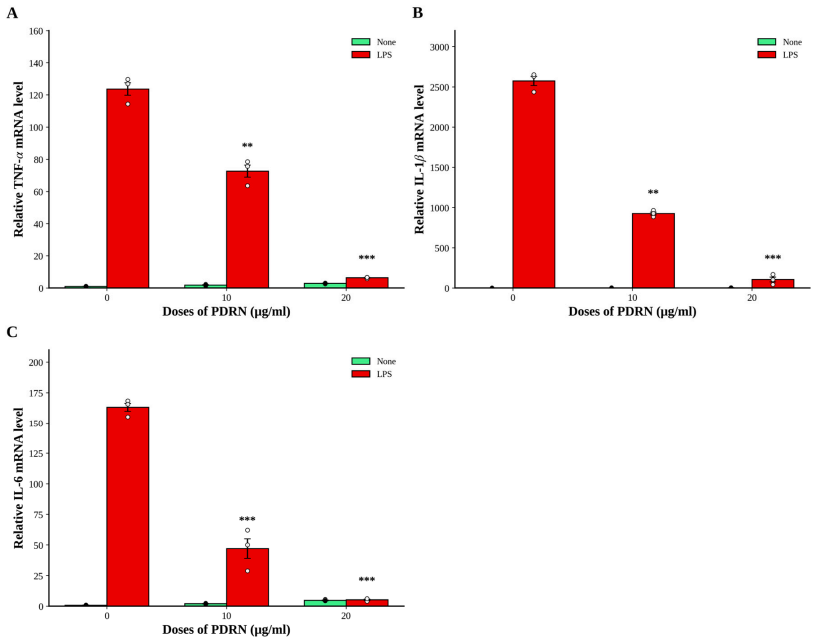

Figure 9. Effects of Ps-PDRN on cytokine mRNA expression in RAW 264.7 cells: (**A**) TNF-α; (**B**) IL-1β; (**C**) IL-6. mRNA levels were measured by real-time PCR and normalized to GAPDH. Data are presented as mean ± SD (n = 3). Two-way ANOVA (LPS × dose) was performed. Post hoc comparisons were conducted using Dunnett's test within the LPS condition only, comparing each Ps-PDRN dose to LPS + 0 μg/mL. ** $p < 0.01$, *** $p < 0.001$ vs. LPS + 0 μg/mL.

4. Discussion

In the present study, we demonstrated for the first time that PDRN derived from *Porphyra* sp. (Ps-PDRN) exerts potent anti-inflammatory effects against LPS-induced ALI in mice. Both intranasal and oral administration attenuated systemic and pulmonary inflammation, supporting the feasibility of non-invasive delivery routes for this marine-derived bioactive compound. ALI is characterized by excessive production of proinflammatory cytokines and chemokines that amplify inflammatory cascades and drive lung injury [14–16]. Consistent with this pathophysiology, Ps-PDRN significantly reduced key cytokines (TNF-α, IL-1β, and IL-6) in BALF and serum and suppressed their mRNA expression in lung tissues. These findings align with prior reports on salmon-derived PDRN, suggesting that PDRN preparations from different marine sources can share anti-inflammatory activity profiles [17,18].

Most previous studies have utilized salmon-derived PDRN (typically 50–1500 kDa) and injection-based administration, with anti-inflammatory effects frequently linked to adenosine A_2A receptor signaling across diverse disease contexts (Supplementary Table S2) [7–10,17,18]. In contrast, Ps-PDRN in the present study spans a broader molecular weight range (5–1000 kDa), and we directly compared intranasal and oral routes in an ALI setting. Although the current work was not designed to define pharmacokinetic determinants, this physicochemical difference may contribute to route-dependent performance and warrants dedicated PK and dose-optimization studies.

Chemokines are central drivers of leukocyte recruitment in ALI, including CC chemokines (MCP-1 and RANTES) and CXC chemokines (CXCL1 and MIP-2), which coordinate monocyte and neutrophil trafficking to inflamed lung tissue [19,20]. Excessive neutrophil infiltration is a hallmark feature contributing to tissue injury through oxidative and proteolytic mechanisms [21]. In our study, Ps-PDRN markedly suppressed chemokine production, and this biochemical suppression was accompanied by improved histopathology, collectively supporting a protective mechanism that includes limiting inflammatory cell recruitment to the lungs.

A clinically relevant observation was the distinct efficacy profile between administration routes (Supplementary Figures S1–S4). In general, oral administration showed a stronger trend in chemokine suppression, whereas intranasal delivery showed advantages for select cytokines, suggesting that local delivery and systemic exposure may differentially modulate inflammatory cascades. Detailed marker-by-marker comparisons are provided in the Supplementary Materials (Supplementary Figures S1–S4). Notably, some markers displayed a non-linear oral dose–response pattern, where the PO-L condition often showed comparable effects to PO-H. This finding should be interpreted cautiously and confirmed by focused dose-ranging studies that incorporate pharmacokinetic endpoints.

The in vitro experiments using RAW 264.7 macrophages further supported a direct anti-inflammatory action of Ps-PDRN under LPS-stimulated conditions. Ps-PDRN dose-dependently inhibited LPS-induced TNF-α and IL-6 production without significant cytotoxicity and suppressed the mRNA expression of proinflammatory cytokines, consistent with transcription-level regulation in an inflammatory context [22,23]. Prior studies have reported that salmon-derived PDRN can inhibit NF-κB and MAPK signaling pathways [24–26]; although signaling was not assessed here, these pathways represent plausible mechanistic candidates for future validation in lung tissue and macrophage compartments.

From a translational standpoint, *Porphyra* sp. is a sustainable and abundant marine resource for PDRN production. Unlike salmon-derived products that rely on animal-sourced raw materials, *Porphyra* can be cultivated at scale, and its long history of dietary use suggests a favorable safety context for development [27,28]. These attributes support

continued investigation of *Porphyra*-derived PDRN as an alternative PDRN source for inflammatory indications.

This study has limitations. First, we did not directly test mechanistic pathways (including A_2A receptor engagement and downstream signaling). Second, Ps-PDRN was evaluated in a prophylactic regimen prior to LPS challenge; therapeutic efficacy in post-insult treatment settings remains to be determined. Third, we used an endotoxin-driven ALI model, and validation in sterile or non-endotoxin lung injury paradigms is warranted. Finally, longer-term safety and pharmacokinetic characterization should be expanded; although supportive systemic safety information is provided from a pre-study 7-day repeated-dose oral evaluation (Supplementary Table S2), route-specific tolerability assessments—particularly local tolerance for intranasal administration—remain necessary.

5. Conclusions

In conclusion, we demonstrated that PDRN derived from *Porphyra* sp. effectively ameliorates LPS-induced acute lung injury in mice through both intranasal and oral administration routes. Ps-PDRN significantly attenuated fever, pulmonary edema, and inflammatory cell infiltration while reducing the production of proinflammatory cytokines and chemokines. Notably, our comparative analysis revealed distinct efficacy profiles between the two administration routes, with oral administration tending to show stronger chemokine suppression, whereas intranasal delivery appeared to provide advantages for select cytokines. The in vitro studies confirmed the direct anti-inflammatory activity of Ps-PDRN on macrophages. These findings support *Porphyra* sp.-derived PDRN as a promising prophylactic candidate against endotoxin-driven acute lung inflammation. Therapeutic efficacy in a post-insult treatment setting remains to be established in future studies. Further studies are needed to elucidate the molecular mechanisms and to evaluate the clinical potential of this marine-derived bioactive compound.

Supplementary Materials: The following supporting information can be downloaded at: https://www.mdpi.com/article/10.3390/cimb48020187/s1.

Author Contributions: Conceptualization, Y.-C.Y.; Methodology, G.-Y.L. and Y.-C.Y.; Investigation, G.-Y.L.; Validation, Y.-C.Y.; Formal analysis, Y.-C.Y.; Resources, J.H. and W.S.L.; Data curation, G.-Y.L., Y.-C.Y. and W.S.L.; Writing—original draft preparation, Y.-C.Y.; Writing—review and editing, G.-Y.L. and Y.-C.Y.; Visualization, Y.-C.Y.; Supervision, Y.-C.Y.; Project administration, Y.-C.Y.; Funding acquisition, Y.-C.Y. and J.H. All authors have read and agreed to the published version of the manuscript.

Funding: This research was supported by the Ministry of SMEs and Startups (MSS) of the Republic of Korea under the 'Industry-University-Research Collaboration R&D Program' (Grant No. RS-2025-02313606), and partly by 'R&D Program for Forest Science Technology (Project No. RS-2023-KF002544)' provided by Korea Forest Service (Korea Forestry Promotion Institute).

Institutional Review Board Statement: The animal study protocol was approved by the Institutional Animal Care and Use Committee of Konyang University (Approval No. P-25-12-A-01 and date of approval 12 July 2025).

Data Availability Statement: The original contributions presented in this study are included in the article/Supplementary Materials. Further inquiries can be directed to the corresponding author.

Acknowledgments: The authors gratefully acknowledge Sang-Seop Lee (Department of Microbiology, Konyang University College of Medicine; ORCID: 0009-0008-2767-2065) for his invaluable expertise in SAS-based advanced statistical analyses and preparation of publication-quality data visualizations. The acknowledged individual has explicitly consented to being acknowledged for the contributions described herein.

Conflicts of Interest: Authors Won Se Lee and Jisung Han were employed by All In One GENETECH Ltd. and DERMARE Co., Ltd. The remaining authors declare that the research was conducted in the absence of any commercial or financial relationships that could be construed as a potential conflict of interest.

References

1. Matthay, M.A.; Zemans, R.L.; Zimmerman, G.A.; Arabi, Y.M.; Beitler, J.R.; Mercat, A.; Herridge, M.; Randolph, A.G.; Calfee, C.S. Acute Respiratory Distress Syndrome. *Nat. Rev. Dis. Primers* **2019**, *5*, 18. [CrossRef]
2. Ma, W.; Tang, S.; Yao, P.; Zhou, T.; Niu, Q.; Liu, P.; Tang, S.; Chen, Y.; Gan, L.; Cao, Y. Advances in acute respiratory distress syndrome: Focusing on heterogeneity, pathophysiology, and therapeutic strategies. *Signal Transduct. Target. Ther.* **2025**, *10*, 75. [CrossRef]
3. Jeyaseelan, S.; Chu, H.W.; Young, S.K.; Worthen, G.S. Transcriptional profiling of lipopolysaccharide-induced acute lung injury. *Infect. Immun.* **2004**, *72*, 7247–7256. [CrossRef] [PubMed]
4. Lv, X.; Lu, X.; Zhu, J.; Wang, Q. Lipopolysaccharide-Induced Acute Lung Injury Is Associated with Increased Ran-Binding Protein in Microtubule-Organizing Center (RanBPM) Molecule Expression and Mitochondria-Mediated Apoptosis Signaling Pathway in a Mouse Model. *Med. Sci. Monit. Int. Med. J. Exp. Clin. Res.* **2020**, *26*, e923172. [CrossRef]
5. Park, B.S.; Lee, J.O. Recognition of Lipopolysaccharide Pattern by TLR4 Complexes. *Exp. Mol. Med.* **2013**, *45*, e66. [CrossRef] [PubMed]
6. Bhatia, M.; Zemans, R.L.; Jeyaseelan, S. Role of Chemokines in the Pathogenesis of Acute Lung Injury. *Am. J. Respir. Cell Mol. Biol.* **2012**, *46*, 566–572. [CrossRef]
7. Galeano, M.; Pallio, G.; Irrera, N.; Mannino, F.; Bitto, A.; Altavilla, D.; Vaccaro, M.; Squadrito, G.; Arcoraci, V.; Colonna, M.R.; et al. Polydeoxyribonucleotide: A Promising Biological Platform to Accelerate Impaired Skin Wound Healing. *Pharmaceuticals* **2021**, *14*, 1103. [CrossRef] [PubMed]
8. Squadrito, F.; Bitto, A.; Altavilla, D.; Arcoraci, V.; De Caridi, G.; De Feo, M.E.; Corrao, S.; Pallio, G.; Sterrantino, C.; Minutoli, L.; et al. The effect of PDRN, an adenosine receptor A2A agonist, on the healing of chronic diabetic foot ulcers: Results of a clinical trial. *J. Clin. Endocrinol. Metab.* **2014**, *99*, E746–E753.
9. Marques, C.; Porcello, A.; Cerrano, M.; Hadjab, F.; Chemali, M.; Lourenço, K.; Hadjab, B.; Raffoul, W.; Applegate, L.A.; Laurent, A.E. From Polydeoxyribonucleotides (PDRNs) to Polynucleotides (PNs): Bridging the Gap Between Scientific Definitions, Molecular Insights, and Clinical Applications of Multifunctional Biomolecules. *Biomolecules* **2025**, *15*, 148. [CrossRef]
10. Miyamoto, E.; Yabuta, Y.; Kwak, C.S.; Enomoto, T.; Watanabe, F. Characterization of vitamin B12 compounds from Korean purple laver (Porphyra sp.) products. *J. Agricult. Food Chem.* **2009**, *57*, 2793–2796. [CrossRef]
11. Jeong, W.; Yang, C.E.; Roh, T.S.; Kim, J.H.; Lee, J.H.; Lee, W.J. Scar Prevention and Enhanced Wound Healing Induced by Polydeoxyribonucleotide in a Rat Incisional Wound-Healing Model. *Int. J. Mol. Sci.* **2017**, *18*, 1698. [CrossRef] [PubMed]
12. Ko, H.S.; Lee, W.S.; Ryu, S.J.; Choi, I.W.; Han, J.S. Antioxidant, anti-inflammatory, and wrinkle-improving effects of PDRN extracted from marine plants. *Asian J. Beauty Cosmetol.* **2025**, *23*, 399–409. [CrossRef]
13. Cao, J.; Wang, J.; Wang, S.; Xu, X. *Porphyra* Species: A Mini-Review of Its Pharmacological and Nutritional Properties. *J. Med. Food* **2016**, *19*, 111–119. [CrossRef] [PubMed]
14. Han, J.-S.; Lee, W.-S. Polydeoxyribonucleotide and Polynucleotide Purified and Extracted from Seaweed. Korean Patent KR 10-2817193, 30 May 2025. Available online: https://www.kipris.or.kr (accessed on 16 January 2026).
15. Kim, T.H.; Heo, S.Y.; Han, J.S.; Jung, W.K. Anti-inflammatory effect of polydeoxyribonucleotides (PDRN) extracted from red alga (*Porphyra* sp.) (Ps-PDRN) in RAW 264.7 macrophages stimulated with *Escherichia coli* lipopolysaccharides: A comparative study with commercial PDRN. *Cell Biochem. Funct.* **2023**, *41*, 889–897. [CrossRef]
16. Long, M.E.; Mallampalli, R.K.; Horowitz, J.C. Pathogenesis of Pneumonia and Acute Lung Injury. *Clin. Sci.* **2022**, *136*, 747–769. [CrossRef]
17. Kumar, V. Toll-Like Receptors in Sepsis-Associated Cytokine Storm and Their Endogenous Negative Regulators as Future Immunomodulatory Targets. *Int. Immunopharmacol.* **2020**, *89*, 107087. [CrossRef]
18. Muniandy, K.; Gothai, S.; Badran, K.M.H.; Suresh Kumar, S.; Esa, N.M.; Arulselvan, P. Suppression of Proinflammatory Cytokines and Mediators in LPS-Induced RAW 264.7 Macrophages by Stem Extract of *Alternanthera sessilis* via the Inhibition of the NF-κB Pathway. *J. Immunol. Res.* **2018**, *2018*, 3430684. [CrossRef]
19. Cheng, Y.; Ma, X.L.; Wei, Y.Q.; Wei, X.W. Potential roles and targeted therapy of the CXCLs/CXCR2 axis in cancer and inflammatory diseases. *Biochim. Biophys. Acta Rev. Cancer* **2019**, *1871*, 289–312. [CrossRef]
20. Conti, P.; Di Gioacchino, M. MCP-1 and RANTES are mediators of acute and chronic inflammation. *Allergy Asthma Proc.* **2001**, *22*, 133–137. [CrossRef]

21. Cargnello, M.; Roux, P.P. Activation and Function of the MAPKs and Their Substrates, the MAPK-Activated Protein Kinases. *Microbiol. Mol. Biol. Rev.* **2011**, *75*, 50–83, Erratum in *Microbiol. Mol. Biol. Rev.* **2012**, *76*, 496. https://doi.org/10.1128/MMBR.00031-10. [CrossRef] [PubMed]
22. Duan, T.; Du, Y.; Xing, C.; Wang, H.Y.; Wang, R.F. Toll-Like Receptor Signaling and Its Role in Cell-Mediated Immunity. *Front. Immunol.* **2022**, *13*, 812774. [CrossRef] [PubMed]
23. Yin, S.; Ding, M.; Fan, L.; Yu, X.; Liang, Z.; Wu, L.; Gao, Z.; Lin, L.; Chen, Y. Inhibition of Inflammation and Regulation of AQPs/ENaCs/Na^+-K^+-ATPase Mediated Alveolar Fluid Transport by Total Flavonoids Extracted from *Nervilia fordii* in Lipopolysaccharide-Induced Acute Lung Injury. *Front. Pharmacol.* **2021**, *12*, 603863. [CrossRef] [PubMed]
24. Guo, Q.; Jin, Y.; Chen, X.; Ye, X.; Shen, X.; Lin, M.; Zeng, C.; Zhou, T.; Zhang, J. NF-κB in Biology and Targeted Therapy: New Insights and Translational Implications. *Signal Transduct. Target. Ther.* **2024**, *9*, 53. [CrossRef]
25. Liu, T.; Zhang, L.; Joo, D.; Sun, S.C. NF-κB Signaling in Inflammation. *Signal Transduct. Target. Ther.* **2017**, *2*, 17023. [CrossRef]
26. Pereira, L.; Critchley, A.T. The COVID-19 Novel Coronavirus Pandemic 2020: Seaweeds to the Rescue? Why Does Substantial, Supporting Research about the Antiviral Properties of Seaweed Polysaccharides Seem to Go Unrecognized by the Pharmaceutical Community in These Desperate Times? *J. Appl. Phycol.* **2020**, *32*, 1875–1877. [CrossRef]
27. MacArtain, P.; Gill, C.I.R.; Brooks, M.; Campbell, R.; Rowland, I.R. Nutritional Value of Edible Seaweeds. *Nutr. Rev.* **2007**, *65*, 535–543. [CrossRef] [PubMed]
28. Wells, M.L.; Potin, P.; Craigie, J.S.; Raven, J.A.; Merchant, S.S.; Helliwell, K.E.; Smith, A.G.; Camire, M.E.; Brawley, S.H. Algae as Nutritional and Functional Food Sources: Revisiting Our Understanding. *J. Appl. Phycol.* **2017**, *29*, 949–982. [CrossRef]